Monitoring the Stimulated Uncapping Process of Gold-Capped Mesoporous Silica Nanoparticles

Ashley E. Augspurger[a], Xiaoxing Sun[a], Brian G. Trewyn[a,b], Ning Fang[a,c]*, and Anthony S. Stender[a,d]*

[a]Department of Chemistry, Iowa State University and The Ames Laboratory, U.S. Department of Energy, Ames, Iowa 50011

[b]Department of Chemistry, Colorado School of Mines, Golden, Colorado 80401

[c]Department of Chemistry, Georgia State University, Atlanta, GA 30302

[d]Department of Chemistry and Biochemistry, Ohio University, Athens, Ohio 45701

ABSTRACT: To establish a new method for tracking the interaction of nanoparticles with chemical cleaving agents, we exploited the optical effects caused by attaching 5-10 nm gold nanoparticles with molecular linkers to large mesoporous silica nanoparticles (MSN). At low levels of gold loading onto MSN, the optical spectra resemble colloidal suspensions of gold. As the gold is removed, by cleaving agents, the MSN revert to the optical spectra typical of bare silica. Time-lapse images of gold-capped MSN stationed in microchannels reveal that the rate of gold release is dependent on the concentration of the cleaving agent. The uncapping process was also monitored successfully for MSN endocytosed by A549 cancer cells, which produce the cleaving agent glutathione. These experiments demonstrate that the optical properties of MSN can be used to directly monitor cleaving kinetics, even in complex cellular settings.

Mesoporous silica nanoparticles (MSN) are a versatile platform for both imaging and drug delivery applications in chemical and biological systems.[1-6] MSN are a popular nanomaterial for applications in these research areas, because they are photo-stable, biocompatible, easy to synthesize, and their surfaces are functionalizable. Because of their porous structure, MSN have a much larger surface area than their non-porous counterparts of the same size, and they provide a large capacity for loading and releasing molecular cargo.

Gold nanoparticles (AuNP) are often incorporated with MSN in order to encapsulate a chemical agent for subsequent delivery with the MSN[7,8] and to increase the MSN density[9], depending on the final application of the material. In the former scenario, a chemical payload is directly loaded into the pores of the MSN via diffusion.[7] Spherical AuNP are separately prepared by functionalizing their surface with stimuli-responsive linker molecules. To cap the MSN pores with these AuNP, the two particle solutions are combined and stirred, and the AuNP attach themselves to the MSN via electrostatic or covalent interaction.[4,5,8] Once the MSN pores are capped, the previously loaded chemical agent is trapped inside the MSN pores unless or until the AuNP are removed. By utilizing disulfide linker molecules, removal of the AuNP can be accomplished by exposing the AuNP-capped MSN to a cleaving agent that will reduce the disulfide bond.

When the primary goal is to increase the density of MSN, gold can be added more directly to MSN by means of plating.[9] Plating is simply the reduction of oxidized gold (Au^{+3}) onto the MSN surfaces, and it is a more straightforward technique to perform than gold-capping. Furthermore, plating provides better control in gold addition, and it allows more gold to be added to the MSN overall than is possible through the AuNP surface functionalization method.[9,10] However, plating also results in the formation of AuNP that are directly deposited onto the silica[10] as opposed to AuNP that are attached to MSN by means of a cleavable linking molecule.

Figure 1 depicts the different classes of MSN particles just described above. Bare MSN have numerous channels that span the entire particle (Figure 1A).[6] Capping places functionalized AuNP on the external surface of MSN, targeting the pore openings (Figure 1B), while plating deposits gold throughout the channels as well as on the exterior of the MSN (Figure 1C). Images collected with transmission electron microscopy (TEM) reveal the differences in appearance of MSN that are bare (Figure 1D) versus gold-plated (Figure 1E). Lastly, MSN that were originally capped with spherical AuNP were imaged before (Figure 1F) and after (Figure 1G) exposure to a chemical cleaving agent. Exposure to the cleaving agent removed all AuNP that were initially present on the MSN.

As a proof of concept that MSN deliver drugs to their intended target, fluorescent dyes such as fluorescein and Ru(bipy) have been previously employed as a payload in control experiments.[4,8,9] No premature release of fluorescent dye from the MSN was observed prior to cleavage of the linker molecules,[8] thus indicating that the payload does indeed reach its target before the dye is released. However, to monitor the uncapping dynamics of individual MSN in real time, particularly in cell experiments, it is advantageous to work with differential interference contrast (DIC) microscopy.[3] DIC microscopy utilizes the principles of polarization and interferometry to generate an image,[3,11-13] and it is a highly effective technique for both single particle spectroscopy[11,12,14] and real time imaging[3,15,16]. It is frequently used in cell studies for taking visible-range widefield images,[3,16,17] oftentimes to accom-

pany fluorescence data. The key benefits for using DIC microscopy include: shallow depth of field, the ability to observe live cells non-intrusively for several hours, no need to work with stains or dyes, no concerns with background fluorescence, and no observation of halo effects.[3,13,16,18]

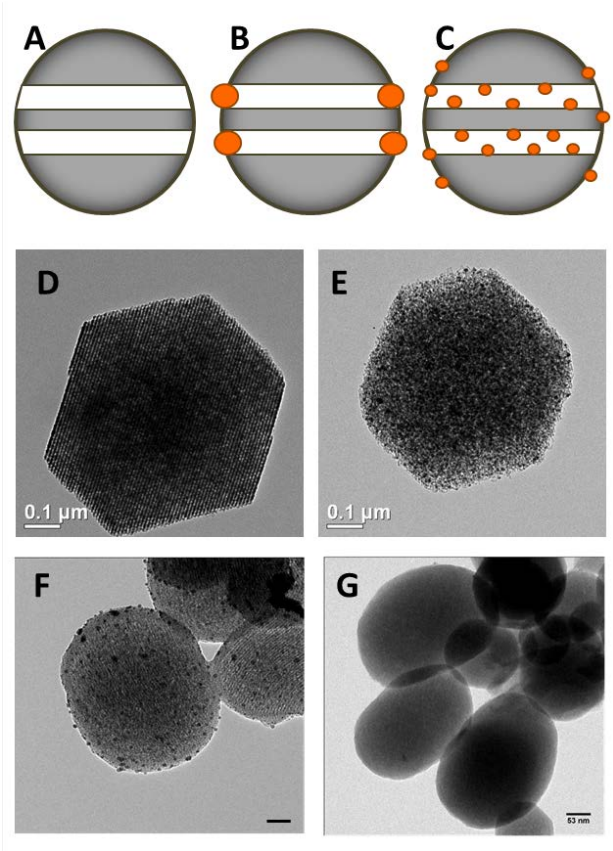

Figure 1. MSN used in this study. A) Cross-section of a bare MSN, revealing its interior channels. B) AuNP-capped MSN with AuNP capping pore openings. C) Gold-plated MSN with gold decorating the interior channels and the MSN exterior. TEM images of D) bare hexagonal MSN, E) gold-plated MSN, F) MSN with AuNP caps before exposure to a cleaving agent and G) MSN with AuNP caps after exposure to a cleaving agent. Scale bars = 100 nm in D, E; 53 nm in F, G.

Characterizing both the gold nanoparticle uncapping kinetics and the drug release kinetics are essential in designing effective drug delivery agents. While the dye release kinetics have been previously measured using fluorescent dye-loaded MSN,[5-7,12,19,20] the AuNP uncapping kinetics have not been quantified experimentally due to the technical challenges of "visualizing" the tiny individual AuNP as they detach from MSN. Studying the AuNP uncapping process is seen as a crucial step towards understanding the stimuli-responsive release of cargo from MSN, because the uncapping process is often the rate limiting step.[19]

The objective of this study was to develop an approach for directly measuring the AuNP uncapping kinetics at the single MSN level. To demonstrate the optical properties of these materials, several batches of MSN were prepared with increasing levels of gold-incorporation, and they were characterized with DIC microscopy. In the next step, the uncapping of AuNP from MSN was monitored in a highly-controlled environment. In brief, AuNP-capped MSN were fixed to the surface of microchannels and monitored with filtered DIC imaging as different concentrations of dithiothreitol (DTT, a disulfide reducing agent) were flowed past the MSN. For the final set of experiments, cultured A549 human lung cancer cells were incubated with AuNP-capped MSN and monitored for several hours as the AuNP were released due to the presence of glutathione, a naturally-produced and cancer-related antioxidant found in these cells that is capable of acting as a cleaving agent.

EXPERIMENTAL PROCEDURES

Nanoparticle Preparation and Characterization.

Synthesis of MSN and spherical AuNP follows the procedures described in detail in earlier publications.[4,7-9] The MSN can be either capped or plated with gold, as explained in the introduction; the plating procedure can be carried out multiple times in succession to add more gold throughout the MSN. In contrast, the AuNP capping process is always performed as a single step, and the spherical AuNP are only attached to the exterior of the MSN and preferentially at the pore openings. As a result, far less gold can be added through the capping process than through plating. Full characterization steps and results including nitrogen sorption analysis, low angle XRD, additional electron micrographs and ICP metal analysis for both MSN with plated gold and MSN with gold caps are available in previously peer-reviewed publications.[4,5,9,21]

Additional Materials.

Glutathione (GSH), dithiothreitol (DTT), and α-lipoic acid were purchased from Sigma Aldrich. Stock solutions were prepared days in advance of each experiment. A549 human lung cancer cells were obtained from American Type Culture Collection (item #CCL-185). To culture the cells, our previously described protocol was followed.[13]

DIC Microscopy.

All imaging was performed on a Nikon Eclipse 80i upright microscope using a 12V-100W halogen lamp as the light source. A 1.40 NA Plan Apo VC oil immersion objective and a 1.40 NA oil condenser, both from Nikon, were also used. Images were collected with a Hamamatsu C11440-10C Orca-Flash 2.8 CMOS camera (1920 × 1440 imaging array with 3.63 μm × 3.63 μm individual pixels). To gather spectroscopic data, images and movies were collected with bandpass filters that were placed into the optical path of the microscope. The bandpass filters were from Thorlabs, and each has a full width at half maximum (FWHM) of 10 nm. Imaging data were analyzed with NIH ImageJ.

Microchannel Fabrication and Imaging.

Microchannels were hand-fabricated from a cleaned standard glass slide (Electron Microscopy Sciences) taped to a 24 x

50 mm glass coverslip (Corning) that was coated with poly-l-lysine (PLL) (Sigma-Aldrich). Into the channel, 20 μL of AuNP-capped MSN were injected and allowed to sit for 15 minutes before imaging, so the nanoparticles could bind to the PLL modified coverslip. During the experiment, the solution, containing either DTT (from Biorad) or GSH (Sigma-Aldrich), was pumped through the channel by means of a gravity feed.

Culturing and Imaging HeLa cells.

A549 cells were cultured 48 hours before imaging with cell culture medium, using our previously published methods.[22] Next the culturing medium was removed and cells were washed with 1X PBS. 24 hours prior to incubation with AuNP-capped MSN, cells were placed in a cell culture medium containing 500μM α-Lipoic acid (Sigma-Aldrich).[23] Cells were kept in the α-lipoic acid culturing medium for 24 hours, and then the AuNP-capped MSN were added. 200 μL of nanoparticles were added to the petri dish with 1 mL of new culturing medium. Cells were incubated for 2 hours to naturally internalize the AuNP-capped MSN.[24] After incubation, the culturing medium and nanoparticle solution were removed, and the cells were washed again with 1X PBS. After the cells were washed with PBS, a slide was prepared for imaging. Two pieces of double sided tape were placed across the slide parallel to one another. Between the two pieces of tape some culturing medium was pipetted, and the glass coverslip was secured on the glass slide with the tape. During imaging, the cell sample was scanned vertically with a computer controlled vertical stage scanner (Sigma Koki, model no. SGSP-60YAM) attached to the fine tune knob of the microscope. A 540 nm (10 nm FWHM) bandpass filter was used to image the cells; the sample was vertically scanned every ten minutes for 3 hours.

Simulation.

To simulate the optical properties associated with differential loading of gold onto MSN via plating (not AuNP capping!), discrete dipole approximation (DDA) was employed. DDSCAT version 7.3 (released in 2013) is a freely-available FORTRAN based code for calculating the scattering and absorption spectra of particles,[25] and it was used to collect all of the simulated data provided.

To describe the MSN particle shape and its multiple configurations embedded with gold, a set of special shape files were created. Each had a hexagonal shape with a flat surface along both the top and bottom edges, in matching with images collected by TEM, shown in Figures 1D and 1E. The underlying MSN structure had a 200 nm diameter and was composed of 43,091 individual dipoles with a spacing set at 5 nm. To simulate the channels that run through the MSN from the top to bottom surface, multiple 5 nm channels were included within the MSN structure. These gaps were evenly distributed throughout the MSN, in keeping with electron microscopy observations. To describe the addition of gold to the MSN structure, dipoles representing gold were added within the channel space. Gold was distributed evenly within the defined channel space. It was assumed that the majority of the gold would be plated within the MSN channels.

Several other variables specified in these experiments also require mention. Since the actual experiments were conducted in aqueous environments, for the simulations, the refractive index (RI) of the surrounding medium was set to that of water (1.33). The dielectric inputs for gold and silica were taken from Johnson and Christy[26] and from Malitson[27], respectively.

RESULTS AND DISCUSSION

To demonstrate their progressive optical properties, MSN were prepared with increasing levels of gold-incorporation through plating and were characterized using DIC microscopy. Two lots of 600 nm hexagonal MSN with 10 nm pore diameters underwent plating to produce 5 nm AuNP on the MSN surfaces; the first lot was exposed to 3 cycles of plating (sample 3X), while the second lot went through 6 cycles (sample 6X). The weight percent (wt%) of gold for the two gold-plated MSN samples were determined by Inductively Coupled Plasma-Mass Spectrometry (ICP-MS). Samples 3X and 6X were determined to be 12 wt% and 30 wt% gold, respectively. For TEM images of the gold plated MSN samples, see SI Figure S1. Absorbance spectra of bare and gold-plated MSN, collected with a Varian Cary 300 UV-Visible spectrophotometer, are available as Figure S2.

Single particle spectroscopy was performed with DIC microscopy and bandpass filters on bare and gold-plated MSN samples (Figure 2). Unlike a dark field image of nanoparticles, in which nanoparticles appear as bright points of light on a dark background, in a DIC image, nanoparticles have both a bright and a dark component, relative to the local "gray" background. Therefore, the DIC-collected data are represented in terms of contrast, which is defined as the difference between a single particle's maximum and minimum optical signal, divided by the average local background signal intensity.[12] The particle spectra presented in Figure 2 are not normalized, but each is the average of three particles. The bare silica spectrum increases in contrast with a decrease in wavelength, as would be expected for a purely-scattering particle. Upon the addition of 12 wt% of AuNP (sample 3X), a distinct peak appears in the spectrum, centered at 550 nm. This profile resembles colloidal gold, and the contrast was improved due to the high absorption provided to the MSN by the presence of gold. Increasing the gold content to 30 wt% (sample 6X) leads to a profile similar to sample 3X but the signal is weaker than the bare silica sample across the entire visible range. To explore this trend further, a sample of MSN exposed to 9 cycles of gold plating was prepared (wt% information for sample 9X not available). The intensity of the 9X spectrum is weaker than that of 6X, and it is relatively flat across the entire visible range. Beyond 640 nm for 9X and 680 nm for 6X, the particles were indistinguishable from the background.

The tendency for MSN to fade and become transparent at increasing levels of gold loading can be explained in terms of RI matching. At 550 nm, the refractive indices of silica and gold are 1.46 [27] and 0.43 [26], respectively. Consequently, as gold incorporation increases, the RI of the MSN should decrease and approach that of the surrounding medium, water. Determining the exact RI of nanoparticles is an ongoing challenge for single nanoparticle research,[28,29] but it is understood that as the difference in RI between nanoparticles and the surrounding medium is minimized,[29] nanoparticles become increasingly transparent (i.e. when imaging, the contrast between the particles and their background approaches zero). A further discussion of the theory surrounding MSN optical

properties as they are incorporated by higher levels of gold, accompanied by computational data, is found in the SI.

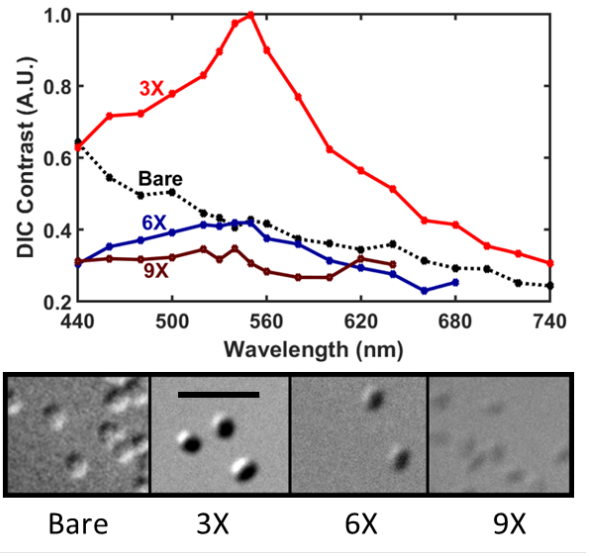

Figure 2. DIC contrast spectra collected from bare and gold-plated MSN with increasing levels of gold incorporation. Each spectral plot represents an averaged value from 3 particles. DIC images of each sample were collected at 540 nm; scale bar inset represents 2.5 um.

Two potential applications present themselves for use with gold-incorporated MSN. The first is to carefully control the amount of gold loading onto the MSN and use the particles for highly accurate refractive index sensing. Such systems are already being explored, primarily in the context of metal-on-metal, plasmonic core-satellite assemblies.[30-32] The other option, and the one explored in further detail below, is to utilize gold-incorporated MSN as real time sensing devices. This can be accomplished by monitoring AuNP-capped MSN as the gold is released from the MSN surface in response to a specific stimulus within either microchannels or cells. In order to pursue this line of experimentation, it was necessary to work specifically with AuNP-capped MSN, since the AuNP are tethered to MSN by stimuli-responsive linker molecules, as opposed to being directly plated onto the MSN.

For the remaining experiments, only AuNP-capped MSN were used. These spherical MSN were monodispersed with an average diameter of 200 nm with 3 nm pore diameters as determined by nitrogen sorption analysis, and 10 nm AuNP were utilized for caps. The AuNP are linked to the MSN through the stimuli-responsive molecule, 3-(propyldisulfanyl) ethylamine. To release the AuNP from MSN, the linker molecule must be reduced at the disulfide bond. The reaction can be facilitated by a number of chemical agents, but the specific agents selected for these experiments were dithiothreitol (DTT) and glutathione (GSH). DTT, also known as Cleland's Reagent, is commonly used at concentrations near 1 mM for the purpose of cleaving AuNP from MSN in cell experiments.[5,6] GSH was selected as a second alternative because of its important connection to cancer at the cellular level, thus it exemplifies an actual chemical that could be exploited to release a cancer-fighting agent delivered with MSN. GSH is a tripeptide normally produced in mammalian cells, but it exists at higher concentrations (5 – 10 mM) in cancerous cells than in non-cancerous cells.[19,33] The GSH level in cells can also be artificially enhanced with the addition of α-lipoic acid to the cell culturing medium.[33]

To prove the validity of monitoring AuNP-release from MSN in real time, three initial experiments were conducted in microchannels. After depositing AuNP-capped MSN inside a microchannel, the channel was filled with water to determine the initial DIC contrast, and then a second solution was flowed through and the particles were monitored in real time.

The first microchannel experiment provided a simple before and after spectral profile of MSN exposed to a flow of 1 mM DTT for 3.5 hours (Figure 3A). The initial profile of AuNP-capped MSN is different from the gold-plated MSN spectra shown in Figure 2, because in this case the AuNP are only on the exterior of MSN. More importantly, the DIC contrast changed significantly during the course of this experiment, with a 20 – 40% decline in contrast at all wavelengths below 600 nm, where the departure of AuNP from MSN would be most noticeable.

Having shown that 1 mM DTT was capable of cleaving the gold from MSN and that a subsequent change in DIC contrast was detectable, a series of additional channel experiments were performed with three different concentrations of DTT: 1 mM, 10 mM, and 100 mM. These data, collected at a wavelength of 540 nm, are shown in Figure 3B. Because of the slow rate at which these reactions proceed, images were recorded at 15 min intervals until the reactions were completed. Flow of the DTT solutions were initiated in each timed trial at time 0 min. Significant changes to DIC contrast were not apparent in any of the trials until 45 min. At a concentration of 100 mM, the reaction appears to be completed in 90 min, while the other two trials reached completion only after 2 hours. The quantitative change in contrast matches closely between the three trials, signifying that each concentration performed with similar effectiveness. Prior experiments with dyes reported that the dye release also occurs over the span of several hours.[4,8]

As a control experiment, and to be certain that the flow of water alone did not cause a change in particle contrast, a third microchannel was prepared with MSN; water not containing a cleaving agent was pumped through this channel. Because no disulfide reducing agent was present in this control experiment, there was no observed change in contrast after 3 hours of solution flow. The results are shown in Figure S3.

For the final set of experiments, it was desired to conduct a test within a complex environment (i.e. cells) using GSH as the reducing agent. In a preliminary test using 5 mM GSH and microchannels, AuNP-capped MSN underwent a change in contrast quite similar to that found with DTT (Figure S4). In a cell experiment, A549 human lung cancer cells were incubated with AuNP-capped MSN. To ensure there was sufficient GSH in the cells, the cells were first incubated with α-lipoic acid, a GSH production enhancer, for 24 h prior to MSN addition. The AuNP-capped MSN were incubated with cells for 3 h prior to imaging. Once the incubation process was completed, the cells were imaged once every 10 min for 3 h at a wavelength of 540 nm. Data from five AuNP-capped MSN tracked during the cell experiment are shown in Figures 4; cell images showing the positions of these five MSN within the cells are included in Figure S5.

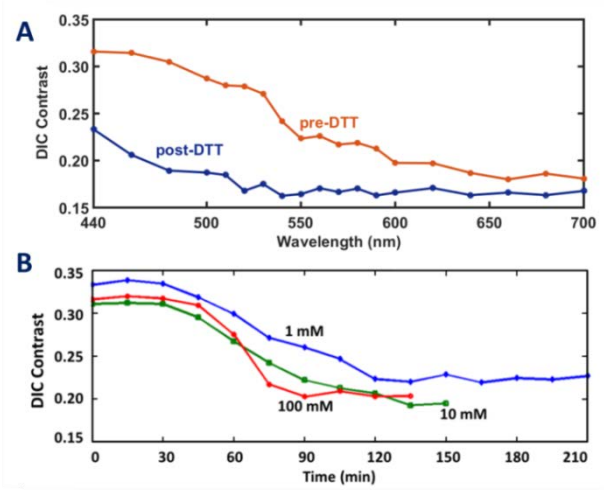

Figure 3. DIC contrast changes associated with loss of AuNP from MSN. A) Spectra of MSN before and after exposure to 1mM DTT for 3.5 hours. B) Time series observation at 540 nm for MSN exposed 1 (blue line), 10 (green), and 100 (red) mM concentrations of DTT.

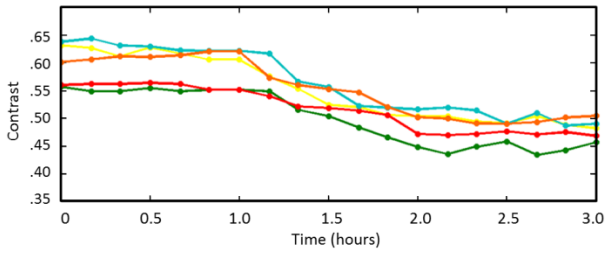

Figure 4. Time series data collected at 540 nm during the cleaving of AuNP from five different MSN via intracellular GSH.

The loss of gold in this case occurred on a time scale remarkably close to that observed in the microchannel experiments. Because the MSN entered the cells by way of endocytosis, the MSN first had to be released from endosomes before they could be exposed to the cytosol, which is where the GSH is located. For the initial 40 min, contrast remained relatively steady. After that time, contrast began to decline until the 2 h mark was reached. From that time onward, the contrast again remained relatively steady for 1 h. Therefore, the loss of gold in this case occurred on a time scale remarkably close to that observed in all of the microchannel experiments. The main conclusion from this experiment is that by tracking the contrast value with DIC microscopy for AuNP-capped MSN in vivo, it is possible to ascertain the timing of AuNP release from the MSN, as well as the location of the MSN within the cells when gold release occurs.

CONCLUSIONS

In conclusion, it has been shown that is possible to monitor the uncapping process of spherical AuNP from MSN by monitoring the MSN optical properties in real time with DIC microscopy. While it is not possible to observe the individual AuNP themselves, due to their extremely small size, the resultant change in DIC contrast displayed by each MSN reveals the dynamic uncapping process. The development of such a technique as described here is especially beneficial for circumstances where tracking with fluorescence is not a viable option or where real time tracking of the AuNP uncapping process is required.

As noted by these experiments, the AuNP release process is not an instantaneous one; rather, gold is released over the course of minutes or hours, and the rate of release is not surprisingly related to the concentration of the cleaving agent. This information should prove helpful in better design of nanoparticle-capped MSN systems that will release a therapeutic agent in a more controlled fashion upon exposure to a targeted stimulus.

ASSOCIATED CONTENT

Supporting Information

The Supporting Information is available free of charge on the ACS Publications website.

The SI section is a single PDF file which includes computational experiment data, and additional figures and experimental results outlined in the main paper.

AUTHOR INFORMATION

Corresponding Authors

* Ning Fang: nfang@gsu.edu
* Anthony Stender: stender@ohio.edu

Author Contributions

The manuscript was written through contributions of all authors. All authors have given approval to the final version of the manuscript.

ACKNOWLEDGMENT

This work is dedicated to the memory of Dr. Victor S.-Y. Lin. A portion of this work was supported by the Director of Science, Office of Basic Energy Sciences, Division of Chemical Sciences, U.S. Department of Energy. The Ames Laboratory is operated for the U.S. Dept. of Energy by Iowa State University under contract #DE-AC02-07CH11358. A.S. acknowledges additional support from start-up funding provided by Ohio University.

REFERENCES

(1) Deodhar, G. V.; Adams, M. L.; Trewyn, B. G. *Biotechnol. J.* **2017**, *12*, 1600408.
(2) Huang, X.; Wu, S.; Ke, X.; Li, X.; Du, X. *ACS Appl. Mat. Inter.* **2017**, *9*, 19638-19645.
(3) Sun, W.; Fang, N.; Trewyn, B. G.; Tsunoda, M.; Slowing, I. I.; Lin, V. S. Y.; Yeung, E. S. *Anal. Bioanal. Chem.* **2008**, *391*, 2119.
(4) Sun, X.; Zhao, Y.; Lin, V. S. Y.; Slowing, I. I.; Trewyn, B. G. *J. Am. Chem. Soc.* **2011**, *133*, 18554-18557.
(5) Torney, F.; Trewyn, B. G.; Lin, V. S. Y.; Wang, K. *Nat. Nanotechnol.* **2007**, *2*, 295-300.

(6) Vivero-Escoto, J. L.; Slowing, I. I.; Trewyn, B. G.; Lin, V. S. Y. *Small* **2010**, *6*, 1952-1967.
(7) Slowing, I. I.; Trewyn, B. G.; Giri, S.; Lin, V. S. Y. *Adv. Func. Mat.* **2007**, *17*, 1225-1236.
(8) Vivero-Escoto, J. L.; Slowing, I. I.; Wu, C.-W.; Lin, V. S. Y. *J. Am. Chem. Soc.* **2009**, *131*, 3462-3463.
(9) Martin-Ortigosa, S.; Valenstein, J. S.; Sun, W.; Moeller, L.; Fang, N.; Trewyn, B. G.; Lin, V. S. Y.; Wang, K. *Small* **2012**, *8*, 413-422.
(10) Zhu, H.; Liang, C.; Yan, W.; Overbury, S. H.; Dai, S. *J. Phys. Chem. B* **2006**, *110*, 10842-10848.
(11) Stender, A. S.; Wang, G.; Sun, W.; Fang, N. *ACS Nano* **2010**, *4*, 7667-7675.
(12) Sun, W.; Wang, G.; Fang, N.; Yeung, E. S. *Anal. Chem.* **2009**, *81*, 9203-9208.
(13) Wang, G.; Sun, W.; Luo, Y.; Fang, N. *J. Am. Chem. Soc.* **2010**, *132*, 16417-16422.
(14) Chen, K.; Lin, C.-C.; Vela, J.; Fang, N. *Anal. Chem.* **2015**, *87*, 4096-4099.
(15) Augspurger, A. E.; Stender, A. S.; Han, R.; Fang, N. *Anal. Chem.* **2014**, *86*, 1196-1201.
(16) Wang, G.; Stender, A. S.; Sun, W.; Fang, N. *Analyst* **2010**, *135*, 215-221.
(17) Ali, M. R. K.; Wu, Y.; Ghosh, D.; Do, B. H.; Chen, K.; Dawson, M. R.; Fang, N.; Sulchek, T. A.; El-Sayed, M. A. *ACS Nano* **2017**, *11*, 3716-3726.
(18) Stender, A. S.; Marchuk, K.; Liu, C.; Sander, S.; Meyer, M. W.; Smith, E. A.; Neupane, B.; Wang, G. F.; Li, J. J.; Cheng, J. X.; Huang, B.; Fang, N. *Chem. Rev.* **2013**, *113*, 2469-2527.
(19) Lai, J.; Shah, B. P.; Garfunkel, E.; Lee, K.-B. *ACS Nano* **2013**, *7*, 2741-2750.
(20) Sauer, A. M.; Schlossbauer, A.; Ruthardt, N.; Cauda, V.; Bein, T.; Bräuchle, C. *Nano Lett.* **2010**, *10*, 3684-3691.
(21) Martin-Ortigosa, S.; Valenstein, J. S.; Lin, V. S. Y.; Trewyn, B. G.; Wang, K. *Adv. Func. Mat.* **2012**, *22*, 3576-3582.
(22) Gu, Y.; Di, X.; Sun, W.; Wang, G.; Fang, N. *Anal. Chem.* **2012**, *84*, 4111-4117.
(23) Lai, J.; Shah, B. P.; Garfunkel, E.; Lee, K.-B. *ACS Nano* **2013**, *7*, 2741-2750.
(24) Gu, Y.; Sun, W.; Wang, G.; Fang, N. *J. Am. Chem. Soc.* **2011**, *133*, 5720-5723.
(25) Draine, B. T.; Flatau, P. J. *J. Opt. Soc. Am. A* **1994**, *11*, 1491-1499.
(26) Johnson, P. B.; Christy, R. W. *Phys. Rev. B* **1972**, *6*, 4370-4379.
(27) Malitson, I. H. *J. Opt. Soc. Am.* **1965**, *55*, 1205-1209.
(28) Kano, H.; Iseda, A.; Ohenoja, K.; Niskanen, I. *Chem. Phys. Lett.* **2016**, *654*, 72-75.
(29) Wang, Z.; Wang, N.; Wang, D.; Tang, Z.; Yu, K.; Wei, W. *Opt. Lett.* **2014**, *39*, 4251-4254.
(30) Prasad, J.; Zins, I.; Branscheid, R.; Becker, J.; Koch, A. H. R.; Fytas, G.; Kolb, U.; Sönnichsen, C. *J. Phys. Chem. C* **2015**, *119*, 5577-5582.
(31) Sebba, D. S.; Mock, J. J.; Smith, D. R.; LaBean, T. H.; Lazarides, A. A. *Nano Lett.* **2008**, *8*, 1803-1808.
(32) Yoon, J. H.; Lim, J.; Yoon, S. *ACS Nano* **2012**, *6*, 7199-7208.
(33) Deng, R.; Xie, X.; Vendrell, M.; Chang, Y.-T.; Liu, X. *J. Am. Chem. Soc.* **2011**, *133*, 20168-20171.

Table of Contents artwork